EJGO European Journal of Gynaecological Oncology

Original Research

Morphological analysis of peritoneal dissemination of ovarian cancer based on levels of carbonyl reductase 1 expression

F. Oyama[1], Y. Asano[2], H. Shimoda[2,3], K. Horie[4], J. Watanabe[4], Y. Yokoayama[1]

[1]Department of Obstetrics and Gynecology, [2]Department of Neuroanatomy, Cell Biology and Histology, [3]Department of Anatomical Science, Graduate School of Medicine, Hirosaki University, Hirosaki, [4]Department of Cellular and Histo-Pathology, Division of Medical Life Science, Hirosaki University Graduate School of Health Science, Hirosaki, Aomori (Japan)

Summary

Purpose of Investigation: When carbonyl reductase 1 (CR1) is highly expressed in human ovarian cancer cells *in vivo*, tumor growth is reported to be inhibited. Conversely, when expression of CR1 decreases, tumor growth, invasion, and metastasis are reported to increase. Thus, the aim of the current study was to examine dynamic changes in ovarian cancer cells under different CR1 expression levels in artificial human peritoneal tissue (AHPT). *Materials and Methods:* Serous ovarian cancer cells with different levels of CR1 expression were produced by transfection of HRA human ovarian carcinoma cells with CR1 DNA or CR1 siRNA. The transfected cells were seeded in AHPT and observed over time until peritoneal development of carcinomatosis. Apoptotic cells in the AHPT were compared using TUNEL staining and fluorescence-based flow cytometry. *Results:* Cells transfected with CR1 DNA or CR1 siRNA did not differ from control cells in terms of their adherence to the mesothelium. After 24 hours, when cells had invaded the tissue below the mesothelium, proliferation of CR1-overexpressing cells was inhibited while proliferation of CR1-suppressing cells increased. At 72 hours, CR1-suppressing cells had invaded the stroma. CR1-overexpressing cells had a markedly higher rate of apoptosis than control or CR1-suppressing cells. Moreover, electron microscopy revealed apoptotic bodies in cells overexpressing CR1. Differences in tumor growth depending on the extent of CR1 expression have been noted *in vivo*, and similar results were obtained in the present *in vitro* model of AHPT. High and low levels of CR1 expression did not affect cell adherence to the mesothelium, but low levels did result in cells invading and proliferating below the mesothelium. *Conclusion:* The present results have also demonstrated that tumor inhibition by CR1 involves an increase in apoptosis.

Key words: Carbonyl reductase 1; Ovarian cancer cells; Artificial human peritoneal tissue; Transfection; Apoptosis.

Introduction

Epithelial ovarian cancer is the most common gynecological cancer and was the 7th leading form of cancer in women in 2008 according to the World Health Organization Global Database [1]. The prognosis for ovarian cancer is closely related to the cancer clinical stage at diagnosis, with Stage III or IV having a poor prognosis. Unfortunately, the disease is often not detected until the advanced stages due to a lack of symptoms during the early stages [2, 3]. Thus, many drugs have been developed to treat ovarian cancer. Although combination chemotherapy including molecularly targeting drugs, such as bevacizumab is thought to be relatively effective against this disease, the five-year survival rate of advanced ovarian cancer patients remains at 20% [2, 4]; hence there is an urgent need for new treatment strategies.

Carbonyl reductase 1 (CR1) is an NADPH-dependent oxidoreductase with broad specificity for carbonyl compounds, which reduces aldehydes and ketones [5]. CR1 is present in a variety of organs, such as the liver, kidney, breast, ovary, and vascular endothelial cells, and its primary function is considered to be controlling fatty acid metabolism [6]. Furthermore, CR1 has been reported to be involved in malignant tumor growth. Suppression of CR1 expression was associated with poor prognosis in uterine endometrial cancer and uterine cervical squamous cell carcinoma [7, 8]. Further, decreased CR1 expression in uterine cervical squamous cell carcinomas promotes tumor growth via epithelial mesenchymal transition [9].

The present authors showed that clofibric acid, a peroxisome proliferator-activated receptor α ligand, increased the expression of CR1 in ovarian cancer tissues [10]. Overexpression of CR1 resulted in reduced microvessel density and induced apoptosis, ultimately inhibiting tumor growth [10]. Decreased CR1 expression is associated with lymph node metastasis and poor prognosis in ovarian cancer [11], and induction of CR1 expression in ovarian tumors leads to a spontaneous decrease in tumor size [12]. Conversely, reducing the level of CR1 expression in a human ovarian cancer cell line promoted tumor growth and increased the frequency of metastasis to the lungs [13]. Moreover, it has been reported that CR1 had anti-tumor potential by activating caspase-8 and caspase-3 via tumor necrosis factor receptor 1, and that this induced apoptosis by inhibiting the inflammation and anti-apoptotic action associated with NF-κB and c-Jun [14]. However, the above results linking CR1 to cell proliferation and invasion were obtained from

Eur. J. Gynaecol. Oncol. - ISSN: 0392-2936
41, n. 3, 2020
doi: 10.31083/j.ejgo.2020.03.5094

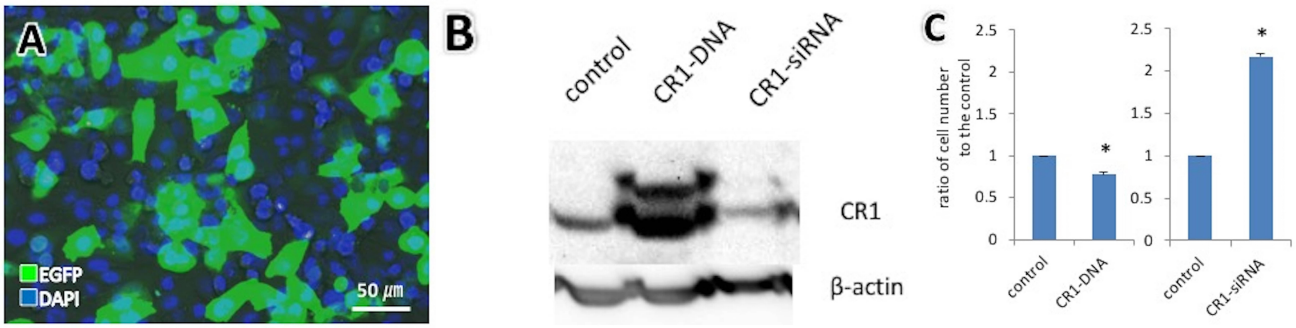

Figure 1. — Effect of CR1 expression levels on ovarian cancer cell proliferation. (A) Fluorescent images (overlay with the phase difference) of HRA cells transfected with the CR1 overexpression construct pCMV6-AC-GFP taken 48 hours post-transfection. (B) CR1 expression levels determined by western blot analysis. β-actin was used as an internal control. (C) Comparison of cell density (as assessed by microscopy) of HRA cells (control), CR1-DNA-transfected HRA cells and CR1-siRNA-transfected HRA cells. * $p < 0.05$ versus the control.

in vivo studies. As a novel approach, the current study applies a three-dimensional artificial human peritoneal tissue (AHPT) containing the lymphatic vascular network that the present authors have recently developed. The AHPT has been developed using a tissue engineering method known as cell-accumulation technique. The engineered tissue displays a structure highly similar to human peritoneal tissue, and can be used to demonstrate the morphological dynamics of cancer peritoneal metastasis [15]. In addition, the present continued studies using AHPT have clearly demonstrated the processes of adhesion, proliferation, and invasion of ovarian cancer cells are characteristic of peritoneal carcinomatosis. Additionally, the present AHPT-peritoneal carcinomatosis model successively showed pathogenesis similar to the disease *in vivo* but in a short period of time, demonstrating its usefulness as an alternative to an animal experiment [16].

In this study, the authors investigated the effect of CR1 expression levels on the proliferation and invasion of ovarian cancer cells using the AHPT ex vivo model.

Materials and methods

Primary cultured neonatal human dermal fibroblasts (NHDFs) and neonatal human dermal lymphatic endothelial cells (HDLECs) were purchased. Primary cultured adult human omentum-derived mesothelial cells (AMCs) were also purchased. HRA cells derived from human epithelial ovarian adenocarcinoma (serous carcinoma) were generously provided by Dr. Y. Kikuchi (National Defense Medical College, Japan) in December 2014. These HRA cells, when subcutaneously or intraperitoneally injected into nude mice have been shown to develop the same histological features as the original tumor [17]. This cell line has been tested for mycoplasma infection and was most recently authenticated by short tandem repeat-polymerase chain reaction at the Department of Bioscience and Laboratory Medicine of Graduate School of Health Science, Hirosaki University in March 2016. NHDFs were cultured in Dulbecco's modified Eagle's medium (DMEM), supplemented with 10% fetal bovine serum (FBS) in 5% CO_2 at 37 °C. HDLECs were cultured in endothelial cell growth medium-2 (EGM-2). AMCs were cultured in collagen type I-coated dishes with mesothelial cell growth medium. HRA cells were cultured in RPMI-1640 supplemented with 10% FBS. Bovine plasma-derived fibronectin (FN) and porcine skin gelatin (G) were purchased. Transwell inserts with a porous polyester bottom (pore size: 0.4 μm) for 24-well culture plates were utilized.

Details on artificial human peritoneal tissue (AHPT) were described in a previous study [15]. AHPT was fabricated on Transwell inserts that were placed in a 24-well cell culture plate containing DMEM supplemented with 10% FBS. Briefly, AHPT is composed of multi-layered 3D tissue consisting of four basal layers of NHDFs, a single layer of HDLECs, four upper layers of NHDFs, and a single top layer of AMCs. NHDFs or HDLECs were coated with fibronectin-gelatin nanofilms as described previously [15]. The pCMV6-AC-GFP vector, which encodes the human CR1, green fluorescent protein (GFP), and ampicillin-resistant gene, was used to optimize and obtain highly efficient transfection. For amplification, pCMV6-AC-GFP was transformed into Escherichia coliDH5α competent cells by heat shock transformation according to standard laboratory protocols. The transformed bacteria were amplified in LB medium containing ampicillin. The plasmids were purified from cultured transformed bacteria using a PureLink HiPure Plasmid Filter Miniprep DNA purification kit according to the manufacturer's protocol. Plasmid DNA (pDNA) was diluted in sterile water at a concentration of 3 μg/μL.

The sequences of small interfering RNA (siRNA) duplexes specific to CR1 were synthesized commercially. CR1 siRNA sense, 5′-AUACGUUCACCACUCUCCCTT-3′ and antisense, 5′-GGGAGAGUGGUGAACGUAUTT-3′ were designed to target different coding regions of the human CR1 mRNA sequence.

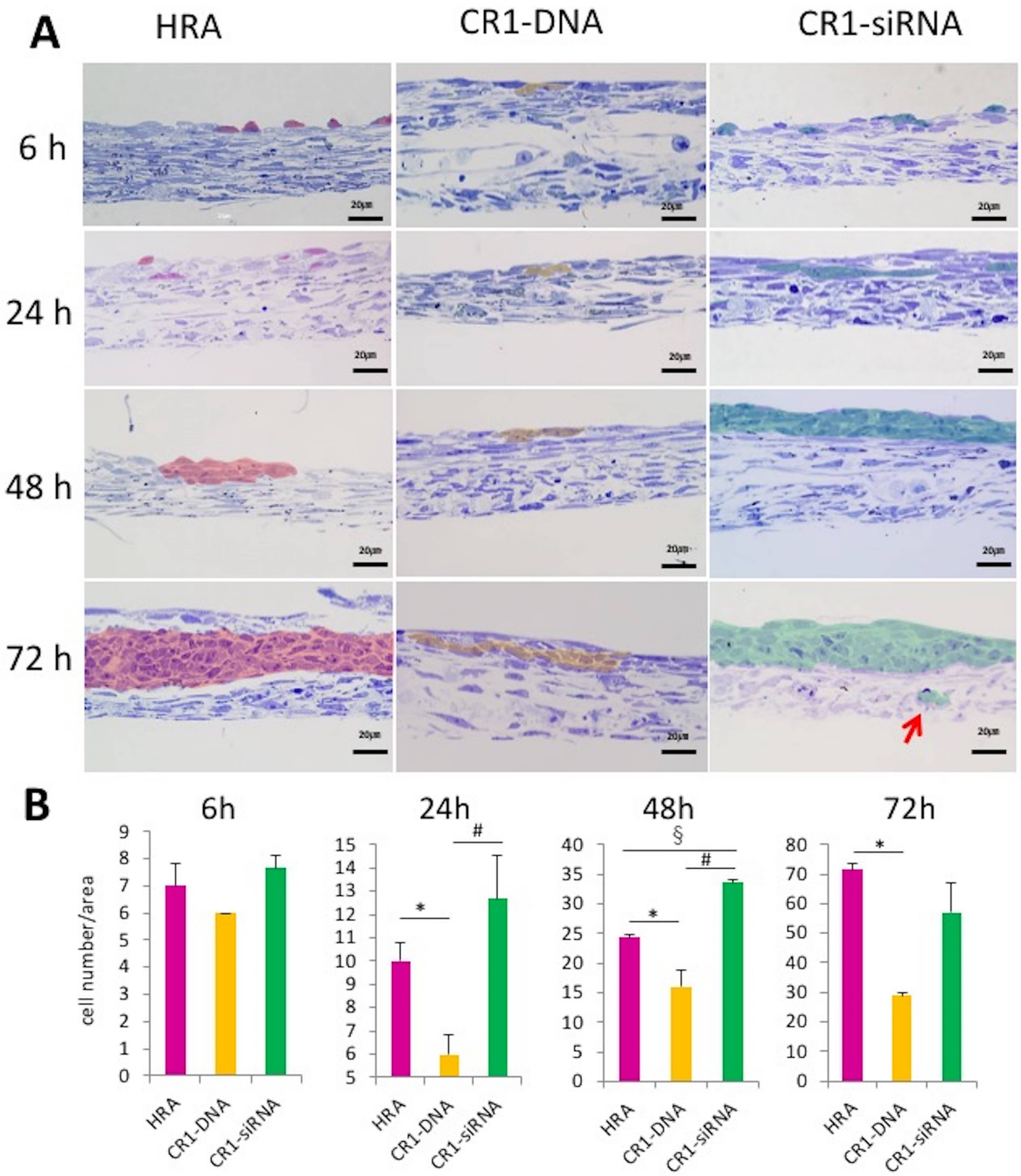

Figure 2. — *In vitro* peritoneal metastasis model comparing overexpression and suppression of CR1. (A) Cross-sections of AHPT seeded with HRA cells (red), CR1-DNA-transfected HRA cells (yellow), and CR1-siRNA-transfected HRA cells (green) stained with toluidine blue. Cell invasion in the stroma-like structure was observed in CR1-siRNA-transfected HRA cells at 72 hours (red arrow). Scale bars; 20 μm. (B) Quantification of HRA cell number. * $p < 0.05$, control HRA versus CR1-DNAtransfected HRA, § $p < 0.05$, control HRA versus CR1-siRNA-transfected HRA, # $p < 0.05$, CR1-DNA-transfected HRA versus CR1-siRNA-transfected HRA.

HRA cells were plated and cultured in 10 mL of RPMI-1640 supplemented with 10% FBS without antibiotics in 10 cm culture dishes and grown until 70–80% confluent for transfection [14]. Lipofectamine 3000 was used for DNA transfection according to the manufacturer's protocol. Briefly, 15 μg of CR1-DNA and 22.5 μL of lipofectamine were each diluted separately in 500 μL of RPMI-1640 and incubated for five minutes at room temperature. Following incubation, the DNA and lipofectamine solutions were combined and incubated for 15 minutes at room tempera-

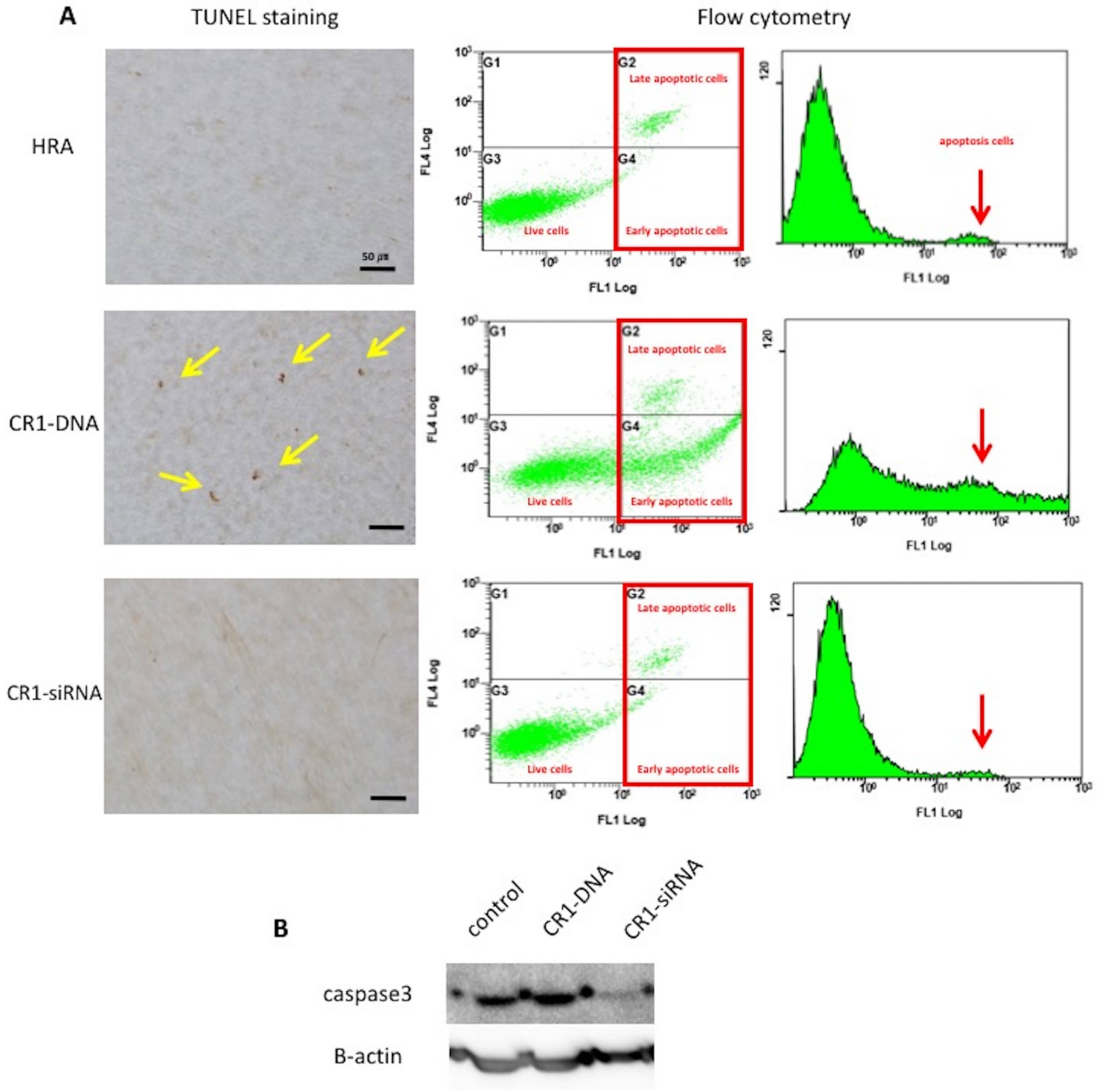

Figure 3. — Effect of CR1 expression levels on apoptosis of ovarian cancer cells in an AHPT model. (A) TUNEL staining of AHPT and fluorescent detection of apoptotic cells 48 hours after seeding either control HRA cells. (B) CR1-DNA-transfected HRA cells. (C) CR1-siRNA-transfected HRA cells. In the microscopy images, yellow arrows show the TUNEL-positive cells (scale bar; 50 μm). On the fluorescence graphs, red boxes and arrows indicate apoptotic cells. (D) Caspase-3 expression in HRA cells, CR1-DNA-transfected HRA cells, and CR1-siRNA-transfected HRA cells. β-actin was used as an internal control.

ture. Finally, 1000 μL of transfection complex was added to a 10-cm culture dish and incubated for 48 hours. The vector without CR1-DNA was used as the control. The control cells were transfected with a mixture of the control vector and lipofectamine by the same method as that described above. The present authors confirmed the expression of the CR1 construct using fluorescence microscopy and western blot analysis.

HRA cells were plated and cultured in 10 mL of RPMI-1640 supplemented with 10% FBS without antibiotics in

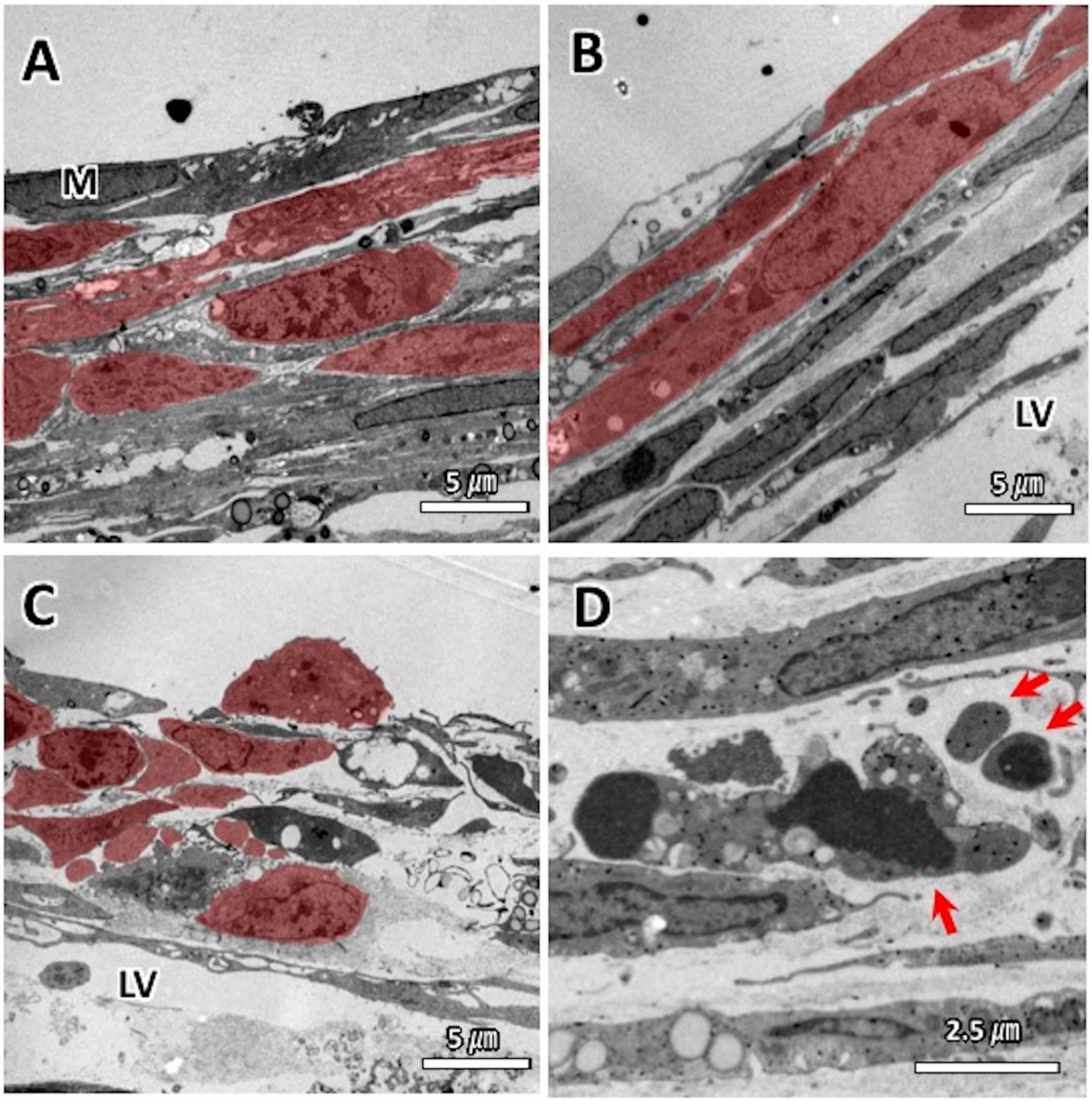

Figure 4. — Transmission electron microscopy (TEM) images showing the effect of CR1 expression in an AHPT model. TEM images are shown of AHPT 48 hours after seeding with either control HRA cells (A), CR1-siRNA-transfected HRA cells (B), or CR1-DNA-transfected HRA cells (C, D). (C) Note the cancer cells have changed to a 'stone wall' shape and display a decrease in cytoplasm (pink color shows cancer cells, scale bar; 5 μm). (D) A higher magnification of AHPT seeded with CR1-DNA-transfected HRA cells. Note the karyorrhexis in cancer cells and presence of apoptotic bodies (red arrows). Scale bar; 2.5 μm. M: mesothelium, LV: lymphatic vessel.

10 cm culture dishes and grown until 30-50% confluent for transfection. Lipofectamine 3000 was used for the siRNA transfection. Briefly, 600 pmol of CR1 siRNA and 30 μL of lipofectamine were each diluted separately in 500 μL of RPMI-1640 and incubated for five minutes at room temperature. Following incubation, the siRNA and lipofectamine solutions were combined and incubated for 20 minutes at room temperature. Finally, 1000 μL of transfection complex was added to each 10 cm culture dish and cultured for 48 hours. The present authors confirmed the effect of the CR1 siRNA using western blot analysis.

HRA cells were cultured in 10 cm dishes as described in the 'cell line and culture' paragraph above. Cell counts were performed during a logarithmic growth phase for 48

hours after transfection of HRA cells with CR1-DNA or CR1-siRNA. To measure viability, cells were stained with 0.3% trypan blue solution. The cell count was performed in triplicate using a hemocytometer and the total cell counts are presented as averages.

Cell lysates were prepared from HRA cells 48 hours after transfection with CR1-DNA or CR1-siRNA. The protein concentration was measured using the Bradford method. The protein samples (10 μg) were electrophoresed through a 12.5% sodium dodecyl sulfate–polyacrylamide gel and subsequently transferred to a nitrocellulose membrane. Non-specific binding was blocked by incubation with 5% skim milk in 20 mM Tris-HCl (pH=7.5, using 0.5 M HCl), or tris-buffered saline (TBS), for one hour at room temperature. After being washed three times with TBS containing 0.05% Tween 20 (TTBS), the blots were probed with the following diluted antibodies for two hours: CR1 at 1:100, caspase-3 at 1:200, and β-actin at 1:1000. β-actin was used as a loading control. Following incubation with primary antibody, the membranes were washed three times with TTBS and incubated for one hour at room temperature with an anti-rabbit IgG horseradish peroxidase (HRP)-linked antibody for CR1 or an anti-mouse IgG HRP-linked antibody for caspase-3 and β-actin. After three washes in TTBS, the membrane was incubated in enhanced chemiluminescence (ECL) western blotting detection reagents for 60 seconds at room temperature. The protein bands on the membrane were visualized using ECL, according to the manufacturer's instructions. The band intensity was analyzed with Molecular Imager, Image Lab v. 3.0.1.

An *in vitro* model of peritoneal metastasis was created using the methods described by Asano *et al.* [15]. Control HRA cells, CR1-DNA-transfected HRA cells, and CR1-siRNA-transfected HRA cells were seeded on AHPT (700 cells/mm2 in 300 μL of DMEM supplemented with 10% FBS). The tissue was collected after 6, 24, 48, and 72 hours and fixed with 4% paraformaldehyde in 0.1 M phosphate buffer (pH 7.4) for light microscopy, or 2.5% glutaraldehyde and 2% paraformaldehyde in 0.1 M phosphate buffer (pH 7.4) for electron microscopy.

Tissues were embedded in paraffin, and 5-μm thick serial tissue sections were prepared on glass slides. For immunohistochemistry, antigen retrieval was performed by boiling the deparaffinized sections in 1 mM EDTA/10 mM Tris-HCl (pH 9.0) using a microwave oven at 500 W for 5 min each. The sections were then treated with 3% normal goat serum-in 0.1 M phosphate buffer (pH 7.4) containing 0.05% Triton X-100 for one hour at room temperature and subsequently incubated overnight with the primary antibodies at 4 °C. The primary antibodies were mouse anti-human podoplanin monoclonal antibody and rabbit anti-pancytokeratin polyclonal antibody. Immunoreactions were visualized by incubating tissues with fluorescence-labeled secondary antibodies, goat anti-mouse IgG conjugated with Alexa-Fluor 594, or goat anti-rabbit IgG conjugated with Alexa-Fluor 488. The specimens were observed using a light microscope or a fluorescence microscope.

For transmission electron microscopy (TEM), tissues were cut into pieces (1 mm^2) and post-fixed in 1% osmium tetroxide in a 0.1 M phosphate buffer. Tissues were then dehydrated and embedded in Epon 812, followed by section preparation using an ultramicrotome. Sections with a thickness of 70 nm were then stained with a 4% uranyl acetate and lead staining solution using conventional methods and observed using a transmission electron microscope.

The area of HRA cells was established based on the morphological characteristics as assessed by light microscopy. Using the light microscope, images (n = 3) were randomly chosen and unified at a size of 150 μm and then cells were counted.

Cell cycle analysis was performed using Cell Meter Apoptotic and Necrotic 'Tricolor Fluorescence' Detection Kit. The HRA cells (control), CR1-DNA-transfected HRA cells, and CR1-siRNA-transfected HRA cells were collected 48 hours after transfection and 5×10^5 cells/tube were centrifuged. Cell were resuspended in 200 μL of Assay Buffer, then 2 μL of Apopxin Green was added, followed by incubation at room temperature for 60 minutes (protected from light). Cells were then diluted by addition of 300 μLAssay Buffer before analysis. A flow cytometer was used to monitor the fluorescence intensity at Ex/Em = 490/525 nm for apoptosis, 550/650 nm for necrosis, and 405/450 nm for healthy cells. A fluorescence microscope was used to quantify Apopxin Green binding (Ex/Em = 490/525 nm), and cell viability was assessed following addition of 7-AAD (Ex/Em = 490/650 nm) or CytoCalcein Violet 450 (Ex/Em = 405/450 nm).

Apoptosis analysis was performed using the In situ Apoptosis Detection Kit. AHPT seeded control HRA cells, CR1-DNA-transfected HRA cells, and CR1-siRNA-transfected HRA cells were collected 48 hours after the first seeding and fixed with 4% paraformaldehyde in 0.1 M phosphate buffer (pH 7.4). The tissues were washed three times with PBS for five minutes and analyzed according to the manufacturer's instructions.

All the statistical analyses were performed using the Student's t test or Welch's *t*-test, and all results with *p*-values < 0.05 were considered to be statistically significant.

Results

CR1-GFP protein was clearly detected in CR1-DNA transfected cells (Figure 1A). Western blot analysis showed that CR1 expression level was much higher in CR1-DNA-transfected cells and lower in CR1-siRNA-transfected cells than in the control cells (Figure 1B). The ratio of cell number compared to the control was 0.78 ± 0.10 in CR1-DNA-transfected cells and 2.17 ± 0.12 in CR1-siRNA-transfected cells (Figure 1C, $p < 0.05$ in both cases).

This study aimed to ascertain whether CR1 expression levels can alter cancer cell proliferation and invasion on AHPT. Figure 2A shows chronological proliferative changes of control, CR1-DNA-transfected, and CR1-

siRNA-transfected HRA cells. At six hours, there was no significant difference in cell number adhering to the surface of the mesothelium between the three groups (Figure 2B). At 24 hours, CR1-DNA-transfected HRA cells displayed significantly reduced proliferation under the mesothelium compared to both the CR1-siRNA-transfected HRA cells and the control cells (Figure 2B, $p < 0.05$). At 48 hours, the number of proliferating cells was again significantly lower for CR1-DNA-transfected HRA cells compared to the other cell groups (Figure 2B, $p < 0.05$), and additionally the CR1-siRNA-transfected HRA cells displayed significantly higher proliferation than the control cells (Figure 2B, $p < 0.05$). At 72 hours, the number of proliferating cells was once again significantly lower in the CR1-DNA-transfected HRA cells than the other two cell groups (Figure 2B, $p < 0.05$). Although there was no difference in the cell number proliferating between CR1-siRNA-transfected HRA cells and the control cells at 72 hours, some of the CR1-siRNA-transfected HRA cells could be observed invading the stroma structure (Figure 2A).

TUNEL-positive cells were found only in the CR1-DNA-transfected HRA cells (Figure 3A). In the fluorescence detection panels, G4 and G2 show early and late apoptotic cells, respectively, whereas G3 shows live cells. In the control cells, the frequency of apoptosis was 5.1% (early apoptosis: 0.6%, late apoptosis: 4.5%, Figure 3A). In the CR1-DNA-transfected cells, the proportion of cells which were apoptotic was 39.1% (early apoptosis: 29.3%, late apoptosis: 9.9%, Figure 3B), while in the CR1-siRNA-transfected cells, the apoptotic frequency was 4.2% (early apoptosis: 1.2%, late apoptosis: 3.0%, Figure 3C). These results showed that apoptosis occurred more notably in the CR1-DNA-transfected cells than in control or CR1-siRNA-transfected cells. Furthermore, western blot analysis revealed an increased expression of caspase-3 in CR1-DNA-transfected HRA cells compared to the other two cell groups (Figure 3B).

A TEM image 48 hours after seeding cells on AHPT showed similar pathological changes in HRA cells (control) and CR1-siRNA-transfected cells (Figure 4A and B). However, the CR1-DNA-transfected cells developed into a 'stone wall' shape and displayed a decrease in cytoplasm (Figure 4C). Evidence of karyorrhexis, such as chromatin condensation and nuclear fragmentation, were found in the CR1-DNA-transfected cells, and the distribution of apoptotic bodies was also evident (Figure 4D).

Discussion

The results of this study showed the difference in peritoneal dissemination of ovarian cancer due to changes in CR1 expression levels using the ex vivo AHPT system. CR1-overexpressing HRA cells suppressed cell proliferation, while CR1-suppressing HRA cells promoted proliferation and invasive activity.

It is well established that CR1 expression levels are related to the prognosis of ovarian cancer. Decreased CR1 expression in epithelial ovarian cancer was associated with retroperitoneal lymph node metastasis and poor survival [11]. Similarly, Murakami *et al.* reported a significant relationship between decreased CR1 expression and progression-free survival as well as overall survival in uterine cervical or endometrial cancer [7, 8]. Nishimoto *et al.* reported that decreased CR1 expression in uterine cervical squamous cell carcinomas promotes tumor growth via epithelial mesenchymal transition [9].

In terms of animal models, Ismail *et al.* reported for the first time that mouse cancer cells in which CR1 was knocked down by an antisense CR1 cDNA acquired a potent metastatic potential [18]. Osawa *et al.* also reported that ovarian cancer cells in which CR1 was knocked down by siRNA showed significantly higher proliferative ability and invasive activity [13].

Contrastingly, malignant tumors derived from mouse ovarian cancer cells with increased CR1 expression by transfection of CR1 cDNA resulted in spontaneous regression [12]. Growth of subcutaneous tumors made by transplantation of human ovarian cancer cells transfected with human CR1 cDNA was significantly inhibited [14]. Furthermore, Kobayashi *et al.* recently reported that administration of a CR1 DNA-dendrimer complex inhibited development of peritoneal dissemination of ovarian cancerin a mouse model and significantly prolonged the survival of mice [19].

Because the aforementioned results were obtained from human patients or animal models, the detailed mechanism of how cancer cells proliferate or invade the peritoneum remains unclear. The authors' previous study using the ex vivo model AHPT demonstrated the adhesion of cancer cells to the mesothelium. Perforation into the mesothelium via cluster formation of proliferating cancer cells, and fragmentation of mesothelial sheets occur as a series of events in our AHPT-peritoneal carcinomatosis model using ovarian cancer cells. In addition, the AHPT-peritoneal carcinomatosis model successively showed pathogenesis similar to the disease *in vivo*, but in a short period of time, suggesting its usefulness as an alternative model to an animal experiment [16]. As shown in Figure 2, CR1-overexpressing HRA cells suppressed cell proliferation and CR1-suppressing HRA cells promoted cell proliferation compared to control cells. In addition, CR1-suppressing HRA cells invaded the stroma structure of AHPT (Figure 2). Osawa *et al.* reported that ovarian cells transfected with CR1 siRNA had a high potential for cell invasion in an *in vitro* experiment [13], supporting the present current result.

The current study showed that TUNEL-positive cells were found only in CR1-overexpressing HRA cells and the distribution of apoptotic cells was much higher in CR1-overexpressing HRA cells than in CR1-suppressing and control cells using flowcytometry. In addition, morphological observation using a TEM showed karyorrhexis in CR1-overexpressing HRA cells, confirming the occurrence of apoptosis. Miura et al. reported that development of

ovarian cancer was inhibited by CR1 overexpression in an animal experiment [14], and suggested that this might be related to the induction of apoptosis [14]. Therefore, in the current study the authors were able to reproduce the mechanism of action of CR1 in promoting apoptosis in cancer cells using the AHPT model.

It remains unexplained why cancer cells with reduced or lacking CR1 expression have strong potential for cell proliferation and invasion. The authors previously showed that CR1 could suppress angiogenesis and induce apoptosis via inactivation of prostaglandin E2 [10]. As shown in Figure 3B, western blot analysis showed high expression of caspase-3 in CR1-overexpressing HRA cells and very weak expression in CR1-suppressing HRA cells, suggesting that low CR1 expression correlates with suppression of apoptosis. In addition, the number of Ki-67 positive cells was significantly higher in CR1-suppressed HRA cells than control (data not shown). Therefore, CR1 suppression is associated with increased proliferation as well as inhibition of apoptosis.

In this study, the authors were unable to identify differences in tight junction integrity, or structural changes such as altered mitochondria or cytoplasmic autophagy using TEM imaging. Because tumor cells could be morphologically identified, more accurate results might be obtained by advances in cell labeling and improvements in DNA transfection efficiency.

In conclusion, an *in vitro* model of peritoneal metastasis using AHPT revealed that CR1 inhibited peritoneal metastasis by reducing the proliferation of ovarian cancer cells via increased apoptosis. Conversely, decreased CR1 expression promotes cell proliferation and invasion in the present *in vitro* model, mirroring the results of previous *in vivo* experiments. These results emphasize the importance of the AHPT-peritoneal carcinomatosis model for future mechanistic insights, as well as confirm CR1 as a potential new gene therapy for ovarian cancer.

Authors' contributions

FO, YA, HS, YY designed the project and experiments. FO, YA, and HS created AHPT. FO and KH performed the experiments. JW pathologically analyzed the data obtained in the current research. FO, YA, HS and KH generated the figures. FO and YY wrote the manuscript. All authors read and approved the final manuscript.

Acknowledgements

This study was supported by a Grant-in-Aid for Cancer Research from the Ministry of Education, Culture, Sports, Science and Technology (Tokyo, Japan) (No. 17K11263 to Dr. Y. Yokoyama).

Conflict of interest

The authors declare that they have no conflict of interests.

Submitted: December 03, 2018
Accepted: January 10, 2019
Published: June 15, 2020

References

[1] Siegel R., Naishadham D., Jemal A.: "Cancer statistics, 2013". *CA Cancer J. Clin.*, 2013, *63*, 11.
[2] Heintz AP., Odicino F., Maisonneuve P., Quinn MA., Benedet JL., Creasman WT., *et al.*: "Carcinoma of the ovary. FIGO 26th Annual Report on the Results of Treatment in Gynecological Cancer". *Int. J. Gynaecol. Obstet.*, 2006, *95*, S161.
[3] Bookman M.A., Brady M.F., McGuire W.P., Harper P.G., Alberts D.S., Friedlander M., *et al.*: "Evaluation of new platinum-based treatment regimens in advanced-stage ovarian cancer: a Phase III Trial of the Gynecologic Cancer Intergroup". *J. Clin. Oncol.*, 2009, *27*, 1419.
[4] Yokoyama Y., Futagami M., Watanabe J., Sato N., Terada Y., Miura F., *et al.*: "Redistribution of resistance and sensitivity to platinum during the observation period following treatment of epithelial ovarian cancer". *Mol. Clin. Oncol.*, 2014, *2*, 212.
[5] Gonzalez-Covarrubias V., Ghosh D., Lakhman SS., Pendyala L., Blanco JG.: "A functional genetic polymorphism on human carbonyl reductase 1 (CBR1 V88I) impacts on catalytic activity and NADPH binding affinity". *Drug Metab. Dispos.*, 2007, *35*, 973.
[6] Wermuth B., Bohren KM., Heinemann G., von Wartburg JP., Gabbay KH.: "Human carbonyl reductase. Nucleotide sequence analysis of a cDNA and amino acid sequence of the encoded protein". *J. Biol. Chem.*, 1988, *263*, 16185.
[7] Murakami A., Fukushima C., Yoshidomi K., Sueoka K., Nawata S., Yokoyama Y., *et al.*: "Suppression of carbonyl reductase expression enhances malignant behaviour in uterine cervical squamous cell carcinoma: carbonyl reductase predicts prognosis and lymph node metastasis". *Cancer Lett.*, 2011, *311*, 77.
[8] Murakami A., Yakabe K., Yoshidomi K., Sueoka K., Nawata S., Yokoyama Y., *et al.*: "Decreased carbonyl reductase 1 expression promotes malignant behaviours by induction of epithelial mesenchymal transition and its clinical significance". *Cancer Lett.*, 2012, *323*, 69.
[9] Nishimoto Y., Murakami A., Sato S., Kajimura T., Nakashima K., Yakabe K., *et al.*: "Decreased carbonyl reductase 1 expression promotes tumor growth via epithelial mesenchymal transition in uterine cervical squamous cell carcinomas". *Reprod. Med. Biol.*, 2018, *17*, 173.
[10] Yokoyama Y., Xin B., Shigeto T., Umemoto M., Kasai-Sakamoto A., Futagami M., *et al.*: "Clofibric acid, a peroxisome proliferator-activated receptor alpha ligand, inhibits growth of human ovarian cancer". *Mol. Cancer Ther.*, 2007, *6*, 1379.
[11] Umemoto M., Yokoyama Y., Sato S., Tsuchida S., Al-Mulla F., Saito Y.: "Carbonyl reductase as a significant predictor of survival and lymph node metastasis in epithelial ovarian cancer". *Br. J. Cancer*, 2001, *85*, 1032.
[12] Wang H., Yokoyama Y., Tsuchida S., Mizunuma H.: "Malignant ovarian tumors with induced expression of carbonyl reductase show spontaneous regression". *Clin. Med. Insights Oncol.*, 2012, *6*, 107.
[13] Osawa Y., Yokoyama Y., Shigeto T., Futagami M., Mizunuma H.: "Decreased expression of carbonyl reductase 1 promotes ovarian cancer growth and proliferation". *Int. J. Oncol.*, 2015, *46*, 1252.
[14] Miura R., Yokoyama Y., Shigeto T., Futagami M., Mizunuma H.: "Inhibitory effect of carbonyl reductase 1 on ovarian cancer growth via tumor necrosis factor receptor signaling". *Int. J. Oncol.*, 2015, *47*, 2173.
[15] Asano Y., Odagiri T., Oikiri H., Matsusaki M., Akashi M., Shimoda H.: "Construction of artificial human peritoneal tissue by cell-accumulation technique and its application for visualizing morphological dynamics of cancer peritoneal metastasis". *Biochem. Biophys. Res. Commun.*, 2017, *494*, 213.
[16] Oikiri H., Asano Y., Matsusaki M., Akashi M., Shimoda H., Yokoayama Y.: "Inhibitory effect of carbonyl reductase 1 against peritoneal progression of ovarian cancer: Evaluation by ex vivo 3D human peritoneal model". *Mol. Biol. Rep.*, 2019, Apr 25. doi: 10.1007/s11033-019-04788-6. [Epub ahead of print]
[17] Kikuchi Y., Kizawa I., Oomori K., Miyauchi M., Kita T., Sugita M., *et al.*: "Establishment of a human ovarian cancer cell line capable of

forming ascites in nude mice and effects of tranexamic acid on cell proliferation and ascites formation". *Cancer Res.*, 1987, *47*, 592.
[18] Ismail E., Al-Mulla F., Tsuchida S., Suto K., Motley P., Harrison P.R., *et al.*: "Carbonyl reductase: a novel metastasis-modulating function". *Cancer Res.*, 2000, *60*, 1173.
[19] Kobayashi A., Yokoyama Y., Osawa Y., Miura R., Mizunuma H.: "Gene therapy for ovarian cancer using carbonyl reductase 1 DNA with a polyamidoamine dendrimer in mouse models". *Cancer Gene Ther.*, 2016, *23*, 24.

Corresponding Author:
Y. YOKOYAMA, M.D.
Department of Obstetrics and Gynecology Graduate School of Medicine, Hirosaki University 5 Zaifu, Hirosaki, 036-8562 (Japan)
e-mail: yokoyama@hirosaki-u.ac.jp